

## Elastic analysis effect of adhesive layer characteristics in steel beam strengthened with a fiber-reinforced polymer plates

Tahar Hassaine Daouadji<sup>\*1,2</sup>, Lazreg Hadji<sup>1</sup>, Mohamed Ait Amar Meziane<sup>1</sup>  
and Hadj Bekki<sup>1,2</sup>

<sup>1</sup>Département de Génie Civil, Université Ibn Khaldoun Tiaret, BP 78 Zaaroura, 14000 Tiaret, Algérie

<sup>2</sup>Laboratoire de Géomatique et Développement Durable, Université Ibn Khaldoun Tiaret, Algérie

(Received October 16, 2015, Revised March 10, 2016, Accepted March 15, 2016)

**Abstract.** In this paper, the problem of interfacial stresses in steel beams strengthened with a fiber reinforced polymer plates is analyzed using linear elastic theory. The analysis is based on the deformation compatibility approach developed by Tounsi (2006) where both the shear and normal stresses are assumed to be invariant across the adhesive layer thickness. The analysis provides efficient calculations for both shear and normal interfacial stresses in steel beams strengthened with composite plates, and accounts for various effects of Poisson's ratio and Young's modulus of adhesive. Such interfacial stresses play a fundamental role in the mechanics of plated beams, because they can produce a sudden and premature failure. The analysis is based on equilibrium and deformations compatibility approach developed by Tounsi (2006). In the present theoretical analysis, the adherend shear deformations are taken into account by assuming a parabolic shear stress through the thickness of both the steel beam and bonded plate. The paper is concluded with a summary and recommendations for the design of the strengthened beam.

**Keywords:** composites plates; interlaminar stresses; steel beam; strengthening; adherend shear deformations; adhesive

---

### 1. Introduction

Strengthening beams and column by bonding plates to their surfaces is an effective method for extending the life of ageing infrastructure. Plate bonding relies critically on the strength of the adhesive joint, which must be designed to have adequate strength. The reliability of structural adhesive joint depends on several factors. These factors include the design, materials and manufacturing methods of the joints as well as accurate analysis of the strength of the structural adhesive joints.

The behaviour of the interface between the steel beam and FRP can influence the performance of hybrid beam and is influenced by many factors such as the properties and geometries of the steel beam, FRP and adhesive layer. The interface transfers the stresses from steel to FRP plate. Therefore, a comprehensive understanding on the stress state and the stress-transfer mechanism of the interface is necessary for the design and application of the hybrid structures. The interfacial

---

\*Corresponding author, Professor, E-mail: [daouadjitahar@gmail.com](mailto:daouadjitahar@gmail.com)

stress of the hybrid beam has been studied by experimental and theoretical methods. The experimental technologies were applied to test the interfacial stresses (Jones *et al.* 1988). However, the experimental test of interfacial stress fields seems to be difficult because of the complicated distribution of local stresses. The analytical studies (Tounsi 2006) tend to develop a closed-form solutions for the interfacial shear and normal stresses. The determination of interfacial stresses has been researched for the last decade for steel or concrete beams bonded with either steel or advanced composite materials. In particular, several closed-form analytical solutions have been developed (Tounsi *et al.* 2009, Touati *et al.* 2015). All these solutions are for linear elastic materials and employ the same key assumption that the adhesive is subject to normal and shear stresses that are constant across the thickness of the adhesive layer. It is this key assumption that enables relatively simple closed-form solutions to be obtained. In the existing solutions, two different approaches have been employed. The interfacial stress of the hybrid beam has been studied by experimental and theoretical methods (Guenaneche *et al.* 2014, Hassaine Daouadji 2013, El mahi *et al.* 2014). The analytical studies (Benyoucef *et al.* 2014, Oller *et al.* 2015, Ziadani *et al.* 2015) tend to develop a closed-form solutions for the interfacial shear and normal stresses.

We can also mention, in addition fiber composite matrix materials, and to reduce the maximum interfacial stress that we can offer plates bonded with properties classified as FGM plates. Is another alternative can be proposed to strengthen the structures that will be addressed in future research, it is therefore the use of functionally graded materials FGM (Abdelhak *et al.* 2015, Tounsi *et al.* 2013, Benferhat *et al.* 2015, Bourada *et al.* 2015, Belabed *et al.* 2014, Hassaine Daouadji 2013, Hebali *et al.* 2014, Ait yahia *et al.* 2015, Ait amar *et al.* 2014, Bennoun *et al.* 2016, Zidi *et al.* 2014, Boudierba *et al.* 2013, Tounsi *et al.* 2013, Bousahla *et al.* 2014), that in order to improve and ensure the material continuity through the thickness of the reinforcing plate, aiming as a parameter in the mechanical characteristics of FGM, all by passing laws adequately mixes to better meet industrial requirements and the environmental condition.

In this paper, the influence of the characteristics of structural adhesives on the interfacial stresses in FRP plated steel beams is investigated theoretically (Bouakaz *et al.* 2014). These investigations are carried out by means of a new analytical method which takes into account the adherend shear deformations (Krouer *et al.* 2013). The importance of including shear-lag effect of the adherends was shown firstly by Tsai *et al.* (1998) in adhesive lap joints. Tounsi (2006) has extended this theory to study concrete beam strengthened by FRP plate. The basic assumption in these two studies is a linear distribution of shear stress across the thickness of the adherends. However, it is well known that in beam theory, this distribution is parabolic through the depth of beam. In the present developed method this later assumption is taken into consideration. The methods predicts stress distributions along the adhesive joint and can be used to analyse failure of the adhesive, or the substrates in the immediate vicinity of the joint, failure modes typically observed in adhesive joints involving metallic or FRP substrates.

## 2. Methods of analysing adhesive joints

Bonded joints have been used since the 1930s, but it is only relatively recently that this technology has been transferred to the construction industry. Adhesive joints in construction are often on a larger scale than those in the automotive or aerospace industries, and behave in different ways. Furthermore, construction projects are one-offs and it is not economic to base design on test

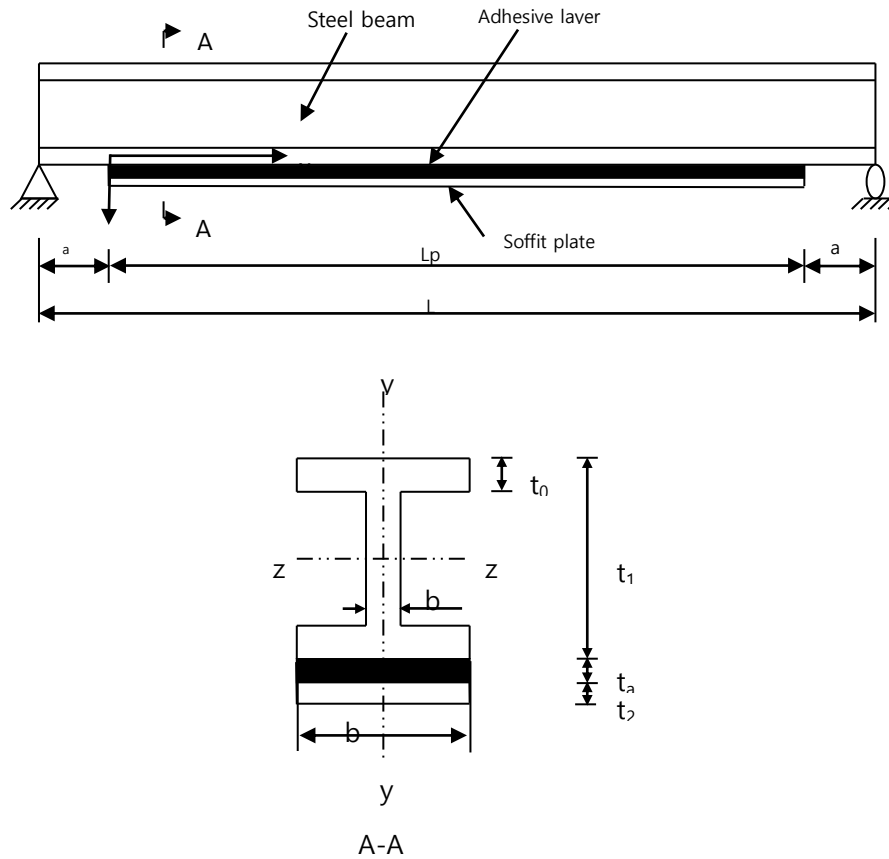


Fig. 1 Simply supported beam strengthened with bonded composite plate

results, unlike other industries with long production runs. Consequently, it is important to have realistic models for the adhesive joint strength. Two approaches can be used to predict the failure of adhesive joints: a stress analysis, or a fracture mechanics approach. Fracture mechanics examines the energy required for unstable crack propagation along the joint; however, this approach has yet to be successfully applied to infrastructure strengthening applications (Herakovich 1998). After the adhesive has cured, the strengthening plate and beam act compositely, with load transferred between them by a combination of shear stresses (parallel to the joint) and peel stresses (normal to the joint). A stress analysis can be used to predict the distributions of shear and peel stress along the strengthened beam, for comparison to the limiting strength of the adhesive joint. Several closed form stress analyses are available that predict the distribution of bond stresses along a plate bonded to a beam. These all assume that the adhesive is linear-elastic, but involve a variety of simplifying assumptions. The motivation behind the approach presented in this paper was the lack of guidance for designing FRP strengthening bonded to metallic structures. The reliability of structural adhesive joint depends on several factors. Among these factors, the adhesive characteristics play an important role in the integrity and reliability of hybrid structure.

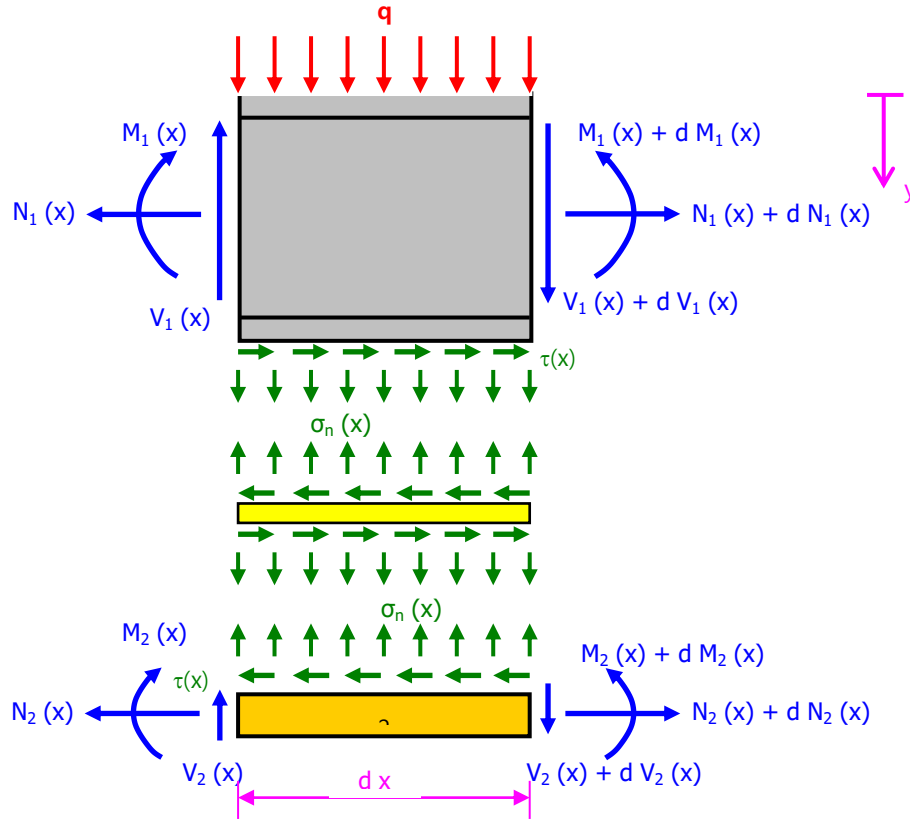


Fig. 2 Forces in infinitesimal element of a soffit-plated beam

### 3. Mathematical formulation of the present method

A differential section  $dx$ , can be cut out from the FRP reinforced steel beam (Fig. 1), as shown in Fig. 2. The composite beam is made from three materials: steel beam, adhesive layer and FRP reinforcement. In the present analysis, linear elastic behaviour is regarded to be for all the materials; the adhesive is assumed to play a role only in transferring the stresses from the concrete to the FRP reinforcement and the stresses in the adhesive layer do not change through the direction of the thickness.

#### 3.1 Basic equation of elasticity

The strains in the steel beam near the adhesive interface can be expressed as

$$\varepsilon_1(x) = \frac{du_1(x)}{dx} = \varepsilon_1^M(x) + \varepsilon_1^N(x) \quad (1)$$

Where  $u_1(x)$  is the longitudinal displacement at the base of steel beam.  $\varepsilon_1^M(x)$  is the strain induced by the bending moment at the adherend 1 and it is written as follow

$$\varepsilon_1^M(x) = \frac{y_1}{E_1 I_1} M_1(x) \quad (2)$$

Where  $M_1(x)$  is the bending moment applied in the steel beam;  $E_1$  is Young's moduli of the steel beam;  $I_1$  is the second moment area;  $y_1$  is the distance from the bottom of adherend 1 to its centroid.  $\varepsilon_1^M(x)$  is the unknown longitudinal strain of the steel beam, at the adhesive interface and it is due to the longitudinal forces. This strain is given as follow

$$\varepsilon_1^N(x) = \frac{du_1^N(x)}{dx} \quad (3)$$

Where  $u_1^N(x)$  represents the longitudinal force induced adhesive displacement at the interface between the steel beam and the adhesive.

To determine the unknown longitudinal strain  $\varepsilon_1^N(x)$  shear deformations of the steel beam is incorporated in this analysis. It is reasonable to assume that the shear stresses, which develop in the adhesive, are continuous across the adhesive-adherend interface. In addition, equilibrium requires the shear stress be zero at the free surface. Using the same methodology developed by Tounsi (2006), Tsai *et al.* (1998), this effect is taken into account. A cubic variation of longitudinal displacement  $U_1^N(x, y)$  through the thickness of adherend 1 is assumed

$$U_1^N(x, y) = A_1(x)y^3 + B_1(x)y + C_1(x) \quad (4)$$

Where  $y$  is a local coordinate system with the origin at the top surface of the upper adherend Fig. 2.

The shear stresses in adherend 1 is given by

$$\sigma_{xy(1)} = G_1 \gamma_{xy(1)} \quad (5)$$

With

$$\gamma_{xy(1)} = \frac{\partial U_1^N}{\partial y} + \frac{\partial W_1^N}{\partial x} \quad (6)$$

$G_1$  is the transverse shear modulus of the adherend 1. Neglecting the variations of transverse displacement  $W_1^N$  (induced by the longitudinal forces) with the longitudinal coordinate  $x$ .

$$\gamma_{xy(1)} \approx \frac{\partial U_1^N}{\partial y} \quad (7)$$

And the shear stresses are expressed as

$$\sigma_{xy(1)} = G_1 (3A(x)y^2 + B(x)) \quad (8)$$

The shear stresses must satisfy the following conditions

$$\sigma_{xy(1)}(x, t_1) = \tau(x) = \tau_a \quad (9)$$

$$\sigma_{xy(1)}(x, 0) = 0 \quad (10)$$

$t_1$ , is the thickness of adherend 1.

Condition (9) follows from continuity and assumption of the uniform shear stresses ( $\tau(x)=\tau_a$ ) through the thickness of adhesive. Condition (10) states there is no shear stresses at the top surface of the adherend 1 (i.e., at  $y=0$ ). These conditions yield

$$\sigma_{xy(1)} = \frac{\tau_a}{t_1^2} y^2 \quad (115)$$

Then with a linear material constitutive relationship the adherend shear strain  $\gamma_1$  for the adherend 1 is written as

$$\gamma_{xy(1)} = \gamma_1 = \frac{\tau_a}{G_1 t_1^2} y^2 \quad (12)$$

The longitudinal displacement functions  $U_1^N$  for the upper adherend, due to the longitudinal forces, is given as

$$U_1^N(y) = U_1^N(0) + \int_0^y \gamma_1(y) dy = U_1^N(0) + \frac{\tau_a}{3G_1 t_1^2} y^3 \quad (13)$$

Where  $U_1^N(0)$  represents the displacement at the top surface of the upper adherend (due to the longitudinal forces).

Note that due to the perfect bonding of the joints, the displacements are continuous at the interfaces between the adhesive and adherends. As a result, the  $u_1^N$  (the adhesive displacement at the interface between the adhesive and upper adherend) should be the same as the upper adherend displacement at the interface. Based on Eq. (13) the  $u_1^N$  can be expressed as

$$u_1^N = U_1^N(y = t_1) = U_1^N(0) + \frac{\tau_a t_1}{3G_1} \quad (14)$$

Using Eq. (14), Eq. (13) can be rewritten as

$$U_1^N(y) = u_1^N + \frac{\tau_a}{3G_1 t_1^2} y^3 - \frac{\tau_a t_1}{3G_1} \quad (15)$$

The longitudinal resultant force,  $N_1$  for the upper adherend, is

$$N_1 = b_1 \int_0^{t_0} \sigma_1^N(y) dy + b_0 \int_{t_0}^{t_1-t_0} \sigma_1^N(y) dy + b_1 \int_{t_1-t_0}^{t_1} \sigma_1^N(y) dy \quad (16)$$

Where  $\sigma_1^N$  is longitudinal normal stress for the upper adherend. By changing these stresses into functions of displacements and substituting Eq. (15) into the displacement, Eq. (16) can be rewritten as

$$N_1 = E_1 b_1 \int_0^{t_0} \frac{dU_1^N}{dx} dy + E_1 b_0 \int_{t_0}^{t_1-t_0} \frac{dU_1^N}{dx} dy + E_1 b_1 \int_{t_1-t_0}^{t_1} \frac{dU_1^N}{dx} dy \quad (17)$$

Hence, the longitudinal strains induced by the longitudinal forces Eqs. (3) can be expressed as

$$\varepsilon_1^N(x) = \frac{du_1^N}{dx} = \frac{N_1}{E_1 A_1} + \frac{1}{12G_1 t_1^2 A_1} \left( b_1 \left[ -t_0^4 - t_1^4 + (t_1 - t_0)^4 + 8t_1^3 t_0 \right] + b_0 \left[ 4t_1^3 (t_1 - 2t_0) - (t_1 - t_0)^4 + t_0^4 \right] \right) \frac{d\tau(x)}{dx} \quad (18)$$

Substituting Eqs. (18) and (2) into Eqs. (1), this latter becomes

$$\begin{aligned}\varepsilon_1(x) &= \frac{du_1(x)}{dx} \\ &= \frac{y_1}{E_1 I_1} M_1(x) + \frac{N_1(x)}{E_1 A_1} + \frac{1}{12 G_1 t_1^2 A_1} \left[ b_1 \left( -t_0^4 - t_1^4 + (t_1 - t_0)^4 + 8 t_1^3 t_0 \right) + b_0 \left( 4 t_1^3 (t_1 - 2 t_0) - (t_1 - t_0)^4 + t_0^4 \right) \right] \frac{d\tau(x)}{dx}\end{aligned}\quad (19)$$

Where  $N(x)$  are the axial forces in each adherend,  $A_1$  the cross-sectional area.

Since the composite laminate is an orthotropic material, its material properties vary from layer to layer. In current study, the laminate theory is used to determine the stress and strain behaviours of the externally bonded composite plate in order to investigate the whole mechanical performance of the composite-strengthened structure. The effective moduli of the composite laminate are varied by the orientation of the fibre directions and arrangements of the laminate patterns. The laminate theory is used to estimate the strain of the symmetrical composite plate, i.e.

$$\varepsilon_x^0 = A_{11}^{-1} N_x \frac{1}{b_2} \quad \text{and} \quad k_x = D_{11}^{-1} M_x \frac{1}{b_2} \quad (20)$$

$[A']=[A^{-1}]$  is the inverse of the extensional matrix  $[A]$ ;  $[D']=[D^{-1}]$  is the inverse of the flexural matrix;  $b_2$  is a width of FRP plate.

Using CLT, the strain at the top of the FRP plate 2 is given as

$$\varepsilon_2(x) = \varepsilon_x^0 - k_x \frac{t_2}{2} \quad (21)$$

Substituting Eq. (20) in (21) gives the following equation

$$\varepsilon_2(x) = \frac{du_2(x)}{dx} = -D_{11}^{-1} \frac{t_2}{2 b_2} M_2(x) + A_{11}^{-1} \frac{N_2(x)}{b_2} \quad (22)$$

Where

$$N_2(x) = N_x \quad \text{and} \quad M_2(x) = M_x \quad (23)$$

$M(x)$ ,  $N(x)$  and  $V(x)$  are the bending moment, axial and shear forces in the adherend.

By adopting the equilibrium conditions of the steel beam, we have:

Along  $x$ -direction:

$$\frac{dN_1(x)}{dx} = -\tau(x) b_2 \quad (24)$$

Where  $\tau(x)$  is shear stress in the adhesive layer.

Along  $y$ -direction:

$$\frac{dV_1(x)}{dx} = -[\sigma_n(x) b_2 + q] \quad (25)$$

Where  $V_1(x)$  is shear force applied in the steel beam;  $\sigma_n(x)$  is normal stress in the adhesive layer and  $q$  is the uniformly distributed load.

Moment equilibrium:

$$\frac{dM_1(x)}{dx} = V_1(x) - \tau(x) b_2 y_1 \quad (26)$$

The equilibrium of the external FRP reinforcement along  $x$ -,  $y$ -direction and moment equilibrium can be also written as:

Along  $x$ -direction:

$$\frac{dN_2(x)}{dx} = \tau(x)b_2 \quad (27)$$

Along  $y$ -direction:

$$\frac{dV_2(x)}{dx} = \sigma_n(x)b_2 \quad (28)$$

Moment equilibrium:

$$\frac{dM_2(x)}{dx} = V_2(x) - \tau(x)b_2 \frac{t_2}{2} \quad (29)$$

Where  $V_2(x)$  is shear force applied in the external FRP reinforcement.

### 3.2 Shear stress distribution along the FRP-beam interface

Here, it is considered that the bending stiffness of the external FRP reinforcement is far less than of the beam to be strengthened and the bending moment in the external FRP reinforcement can be neglected for simplicity in the derivation of shear stress.

The shear stress in the adhesive can be expressed as follows

$$\tau(x) = K_s \Delta u(x) = K_s [u_2(x) - u_1(x)] \quad (30)$$

Where  $K_s$  is shear stiffness of the adhesive per unit length and can be deduced as

$$K_s = \frac{\tau(x)}{\Delta u(x)} = \frac{\tau(x)}{\Delta u(x)/t_a} \frac{1}{t_a} = \frac{G_a}{t_a} \quad (31)$$

$\Delta u(x)$  is relative horizontal displacement at the adhesive interface;  $G_a$  is the shear modulus in the adhesive and  $t_a$  is the thickness of the adhesive.

Substituting Eqs. (19) and (22) into Eq. (30) and differentiating the resulting equation once yields

$$\frac{d\tau(x)}{dx} = K_s \left[ \frac{-y_2}{b_2} D'_{11} M_2(x) + \frac{A'_{11}}{b_2} N_2(x) - \frac{y_1}{E_1 I_1} M_1(x) - \frac{N_1(x)}{E_1 A_1} - \frac{1}{12 G_1 t_1^2 A_1} \left( b_1 [-t_0^4 - t_1^4 + (t_1 - t_0)^4 + 8t_1^3 t_0] + b_0 [4t_1^3 (t_1 - 2t_0) - (t_1 - t_0)^4 + t_0^4] \right) \frac{d\tau(x)}{dx} \right] \quad (32)$$

Assuming equal curvature in the beam and the FRP plate, the relationship between the moments in the two adherends can be expressed as

$$M_1(x) = R M_2(x) \quad (33)$$

With

$$R = \frac{E_1 I_1 D'_{11}}{b_2} \quad (34)$$

Moment equilibrium of the differential segment of the plated beam in Fig. 2 gives

$$M_T(x) = M_1(x) + M_2(x) + N(x)[y_1 + y_2 + t_a] \quad (35)$$

Where,  $M_T(x)$  is the total applied moment and from Eqs. (24) and (27), the axial forces are given as

$$N_1(x) = -N(x) = -b_2 \int_0^x \tau(x) \quad \text{and} \quad N_2(x) = N(x) = b_2 \int_0^x \tau(x) \quad (36)$$

The bending moment in each adherend, expressed as a function of the total applied moment and the interfacial shear stress, is given as

$$M_1(x) = \frac{R}{R+1} \left[ M_T(x) - b_2 \int_0^x \tau(x)(y_1 + y_2 + t_a) dx \right] \quad (37)$$

And

$$M_2(x) = \frac{1}{R+1} \left[ M_T(x) - b_2 \int_0^x \tau(x)(y_1 + y_2 + t_a) dx \right] \quad (38)$$

The first derivative of the bending moment in each adherend gives

$$\frac{dM_1(x)}{dx} = \frac{R}{R+1} [V_T(x) - b_2 \tau(x)(y_1 + y_2 + t_a)] \quad (39)$$

And

$$\frac{dM_2(x)}{dx} = \frac{1}{R+1} [V_T(x) - b_2 \tau(x)(y_1 + y_2 + t_a)] \quad (40)$$

Differentiating Eq. (32)

$$\begin{aligned} \frac{d^2 \tau(x)}{dx^2} = & K_S \left( \frac{A'_{11}}{b_2} \frac{dN_2(x)}{dx} - \frac{y_2}{b_2} D'_{11} \frac{dM_2(x)}{dx} - \frac{y_1}{E_1 I_1} \frac{dM_1(x)}{dx} - \frac{1}{E_1 A_1} \frac{dN_1(x)}{dx} \right) - \\ & \frac{K_S}{12 G_1 t_1^2 A_1} \left[ b_1 \left( (t_1 - t_0)^4 - t_0^4 - t_1^4 + 8t_1^3 t_0 \right) + b_0 \left( 4t_1^3 (t_1 - 2t_0) - (t_1 - t_0)^4 + t_0^4 \right) \right] \frac{d^2 \tau(x)}{dx^2} \end{aligned} \quad (41)$$

Substitution of the shear forces (Eqs. (39) and (40)) and axial forces Eq. (36) into Eq. (41) gives the following governing differential equation for the interfacial shear stress.

$$\frac{d^2 \tau(x)}{dx^2} - K_1 b_2 \left( \frac{(y_1 + y_2)(y_1 + y_2 + t_a)}{E_1 I_1 D'_{11} + b_2} + A'_{11} + \frac{b_2}{E_1 A_1} \right) \tau(x) + K_1 \left( \frac{(y_1 + y_2) D'_{11}}{E_1 I_1 D'_{11} + b_2} \right) V_T(x) = 0 \quad (42)$$

Where

$$K_1 = \frac{1}{\left( \frac{t_a}{G_a} + \frac{t_1}{4G_1} \xi \right)} \quad (43)$$

and  $\xi$  is a geometrical coefficient which is given as

$$\xi = \frac{1}{3A_1 t_1^3} \left[ b_1 \left( -t_0^4 - t_1^4 + (t_1 - t_0)^4 + 8t_0 t_1^3 \right) + b_0 \left( 4t_1^3 (t_1 - 2t_0) - (t_1 - t_0)^4 + t_0^4 \right) \right] \quad (44)$$

For a rectangular section ( $b_1=b_0$ ),  $\zeta=1$ , however, for I-beam section (present case) we have  $\zeta<1$ .

For simplicity, the general solutions presented below are limited to loading which is either concentrated or uniformly distributed over part or the whole span of the beam, or both. For such loading,  $d^2V_T(x)/dx^2=0$ , and the general solution to Eq. (42) is given by

$$\tau(x) = B_1 \cosh(\lambda x) + B_2 \sinh(\lambda x) + m_1 V_T(x) \quad (45)$$

Where

$$\lambda^2 = K_1 b_2 \left( \frac{(y_1 + y_2)(y_1 + y_2 + t_a)}{E_1 I_1 D'_{11} + b_2} + A'_{11} + \frac{b_2}{E_1 A_1} \right) \quad (46)$$

And

$$m_1 = \frac{K_1}{\lambda^2} \left( \frac{(y_1 + y_2) D'_{11}}{E_1 I_1 D'_{11} + b_2} \right) \quad (47)$$

$B_1$  and  $B_2$  are constant coefficients determined from the boundary conditions.

In the present study, a simply supported beam is investigated which is subjected to a uniformly distributed load.

Considering the boundary conditions:

1. Due to symmetry, the shear stress at mid-span is zero, i.e.

$$\tau\left(\frac{L_p}{2}\right) = B_1 \cosh\left(\lambda \frac{L_p}{2}\right) + B_2 \sinh\left(\lambda \frac{L_p}{2}\right) + m_1 V_T\left(\frac{L_p}{2}\right) = 0 \quad (48)$$

Where  $L_p$  is the length of the FRP plate (see Fig. 1).

2. At the end of the FRP plate, the longitudinal force [ $N_1(0)=N_2(0)$ ] and the moment  $M_2(0)$  are zero. As a result, the moment in the section at the plate curtailment is resisted by the beam alone and can be expressed as

$$M_1(0) = M_T(0) = \frac{qa}{2}(L-a) \quad (49)$$

Applying the above boundary condition in Eq. (30)

$$\frac{d\tau(x=0)}{dx} = -m_2 M_T(0) \quad \text{avec} \quad m_2 = \frac{K_1 y_1}{E_1 I_1} \quad (50)$$

From the above three equations

$$B_2 = \frac{-m_2 qa}{2\lambda}(L-a) + \frac{m_1}{\lambda} q \quad (51)$$

$$B_1 = -B_2 \tanh\left(\frac{\lambda L_p}{2}\right); \quad V_T\left(\frac{L_p}{2}\right) = 0 \quad (52)$$

For practical cases  $\frac{\lambda L_p}{2} > 10$  and as a result  $\tanh\left(\frac{\lambda L_p}{2}\right) \approx 1$ . So the expression for  $B_1$  can be simplified to

$$B_1 = -B_2 \quad (53)$$

Substitution of  $B_1$  and  $B_2$  into Eq. (45) gives an expression for the interfacial shear stress at any point

$$\tau(x) = \left( \frac{m_2 a}{2} (L - a) - m_1 \right) \frac{q e^{-\lambda x}}{\lambda} + m_1 q \left( \frac{L}{2} - a - x \right) \quad 0 \leq x \leq L_p \quad (54)$$

Where  $q$  is the uniformly distributed load and  $x$ ,  $a$ ,  $L$  and  $L_p$  are defined in Fig. 1.

In the case where the beam is subjected to a two symmetric point loads, the general solution for the interfacial shear stress is given by the following expressions Tounsi (2006)

$$a < b : \quad \tau(x) = \begin{cases} \frac{m_2}{\lambda} P a e^{-\lambda x} + m_1 P \cosh(\lambda x) e^{-k} & 0 \leq x \leq (b - a) \\ \frac{m_2}{\lambda} P a e^{-\lambda x} + m_1 P \sinh(k) e^{-\lambda x} & (b - a) \leq x \leq \frac{L_p}{2} \end{cases} \quad (55)$$

$$a > b : \quad \tau(x) = \frac{m_2}{\lambda} P b e^{-\lambda x} \quad 0 \leq x \leq L_p \quad (56)$$

Where  $P$  is the concentrated load and  $k = \lambda(b - a)$ . The expression of  $m_1$  and  $m_2$  takes into considerations the shear deformation of adherends.

#### 4. Numerical verification and discussions

The present analytical solution is verified in this section by comparing its predictions with experimental results obtained by Jones *et al.*, with analytical solutions by Smith and Teng 2001, Tounsi 2006, Yang and Wu 2007 and Hassaine Daouadji 2013.

##### 4.1 Comparison with experimental results

To validate the present method, a rectangular section ( $\xi=1$ ) is used here. One of the tested beams bonded with steel plate by Jones *et al.* (1988), beam F31, is analysed here using the present improved solution. The beam is simply supported and subjected to four-point bending, each at the third point. The geometry and materials properties of the specimen are summarized in Table 1.

The interfacial shear stress distributions in the beam bonded with a soffit steel plate under the applied load 180 kN in Fig. 3, are compared between the experimental results and those obtained by the present method. As it can be seen from Fig. 3, the comparison shows encouraging agreement with the experimental results.

##### 4.2 Comparison with approximate solutions

The present simple solution is compared, in this section, with some approximate solutions

Table 1 Dimensions and material properties

Concrete	$b_1=155$ mm	$t_1=225$ mm	$E_1=31000$ MPa
Steel	$b_2=125$ mm	$t_2=6$ mm	$E_2=200000$ MPa
Adhesive	$b_a=123$ mm	$t_a=1.5$ mm	$E_a=280$ MPa , $G_a=108$ MPa

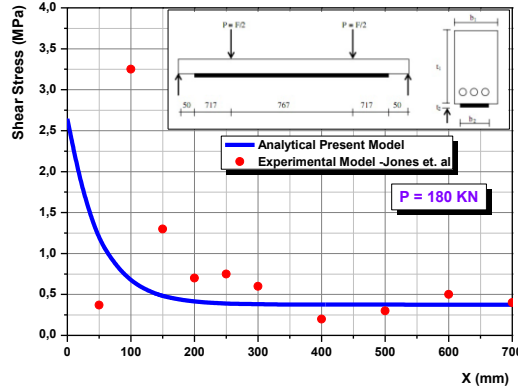


Fig. 3 Comparison of interfacial shear stress of the steel plated RC beam with the experimental results from Jones *et al.*

Table 2 Geometric and material properties

Component	Width (mm)	Depth (mm)	Young's modulus (MPa)	Poisson's ratio	Shear modulus MPa
RC beam	$b_1=200$	$t_1=300$	$E_1=30\ 000$	0.18	-
Adhesive layer RC beam	$b_a=200$	$t_a=4$	$E_a=3000$	0.35	-
GFRP plate (bonded RC beam)	$b_2=200$	$t_2=4$	$E_2=50\ 000$	0.28	$G_{12}=5000$
GFRP plate (bonded steel beam)	$b_1=150$	$t_2=2$	$E_2=50\ 000$	0.28	$G_{12}=5000$
GFRP plate (bonded Aluminium beam)	$b_2=20$	$t_2=2$	$E_2=50\ 000$	0.28	$G_{12}=5000$
CFRP plate (bonded RC beam)	$b_2=200$	$t_2=4$	$E_2=140\ 000$	0.28	$G_{12}=5000$
CFRP plate (bonded steel beam)	$b_1=150$	$t_2=2$	$E_2=140\ 000$	0.28	$G_{12}=5000$
CFRP plate (bonded Aluminium beam)	$b_2=20$	$t_2=2$	$E_2=140\ 000$	0.28	$G_{12}=5000$
Steel plate (bonded RC beam)	$b_2=200$	$t_2=4$	$E_2=200\ 000$	0.3	
Aluminium plate (bonded RC beam)	$b_2=200$	$t_2=4$	$E_2=65\ 300$	0.3	
Aluminium beam (wall thickness 2mm)	$b_1=20$	$t_2=30$	$E_2=65\ 300$	0.3	
Adhesive layer (Aluminium beam)	$b_2=20$	$t_2=2$	$E_2=2\ 000$	0.35	
Steel I- beam (IPE300)	$b_1=150$	$t_1=300$	$E_2=200\ 000$	0.3	

available in the literature. These include Smith and Teng (2001), Tounsi (2006), Yang and Wu (2007), Hassaine Daouadji (2013) solutions uniformly distributed loads. A comparison of the interfacial shear and normal stresses from the different existing closed-form solutions and the present solution is undertaken in this section. An undamaged beams bonded with GFRP, CFRP, Steel and Aluminium plate soffit plate is considered. The beam is simply supported and subjected to a uniformly distributed load. A summary of the geometric and material properties is given in Table 2. The results of the peak interfacial shear and normal stresses are given in Table 3 for the beams strengthened by bonding GFRP, CFRP, Steel and Aluminium plate. As it can be seen from the results, the peak interfacial stresses assessed by the present theory are smaller compared to those given by Smith and Teng (2001), Tounsi (2006), Yang and Wu (2007), Hassaine Daouadji (2013) solutions. This implies that adherend shear deformation is an important factor influencing

Table 3 Comparison of peak interfacial shear and normal stresses (MPa): Uniformly Distributed Load- UDL

Reinforced Concrete Beam bonded with a thin plate subjected to a uniformly distributed load									
Model	RC beam with CFRP plate		RC beam with GFRP plate		RC beam with steel plate		RC beam with aluminum plate		
	Shear	Normal	Shear	Normal	Shear	Normal	Shear	Normal	
Present Model	1.998	1.188	1.121	0.913	2.340	1.282	1.439	1.002	
Tounsi <i>et al.</i> (2009)	1.968	1.169	1.194	0.899	2.304	1.261	1.417	0.985	
Smith and Teng (2001)	2.740	1.484	1.975	1.244	3.696	1.713	1.973	1.251	
Hassaine Daouadji (2013)	1.962	1.162	1.108	0.893	2.297	1.253	1.413	0.980	
Yang and Wu (2007)	2.168	1.225	1.255	1.112	2.539	1.321	1.561	1.033	
Steel Beam bonded with a thin plate subjected to a uniformly distributed load									
Model	Steel beam with CFRP plate			Steel beam with GFRP plate					
	Shear Stress		Normal Stress	Shear Stress		Normal Stress			
Present Model	2.385		1.355	1.477		1.055			
Tounsi <i>et al.</i> (2009)	2.349		1.332	1.454		1.037			
Yang and Wu (2007)	2.580		1.397	1.597		1.087			
Hassaine Daouadji (2013)	2.342		1.325	1.459		1.031			
Smith and Teng (2001)	3.270		1.691	2.025		1.316			
Aluminium Beam bonded with a thin plate subjected to a uniformly distributed load									
Model	Aluminium beam with CFRP plate			Aluminium beam with GFRP plate					
	Shear Stress		Normal Stress	Shear Stress		Normal Stress			
Present Model	1.610		0.889	0.903		0.683			
Tounsi <i>et al.</i> (2009)	1.586		0.875	0.962		0.672			
Yang and Wu (2007)	1.748		0.917	0.987		0.832			
Hassaine Daouadji (2013)	1.580		0.869	0.891		0.667			
Smith and Teng (2001)	2.091		1.081	1.172		0.980			

the adhesive interfacial stresses distribution.

Fig. 4 plots the interfacial shear and normal stresses near the plate end for the example steel bonded with a CFRP plate for the uniformly distributed load case. Overall, the predictions of the different solutions agree closely with each other. The interfacial normal stress is seen to change sign at a short distance away from the plate end. The present analysis gives lower maximum interfacial shear and normal stresses than those predicted by Tounsi 2006, indicating that the inclusion of adherend shear deformation effect in the beam and soffit plate leads to lower values of  $\sigma_{\max}$  and  $\tau_{\max}$ . However, the maximum interfacial shear and normal stresses given by Tounsi 2006 method's is lower than the results computed by the present solution. This difference is due to the assumption used in the present theory which is in agreement with the beam theory. Hence, it is apparent that the adherend shear deformation reduces the interfacial stresses concentration and thus renders the adhesive shear distribution more uniform. The interfacial normal stress is seen to change sign at a short distance away from the plate end.

The results of the peak interfacial shear and normal stresses are given in Table 3 for the RC beam with a GFRP, CFRP, Steel and Aluminum soffit plate. Table 3 shows that, for the UDL case,

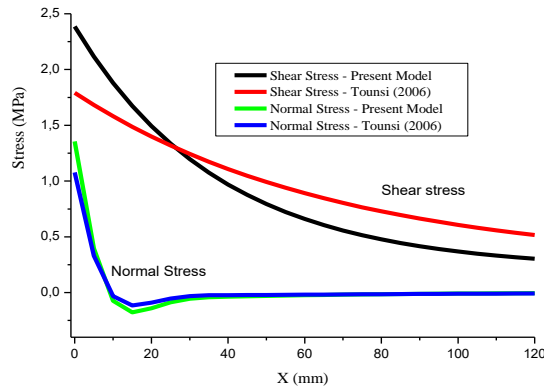


Fig. 4 Comparison of interfacial shear and normal stresses for an RC beam with a bonded CFRP soffit plate subjected to a uniformly distributed load

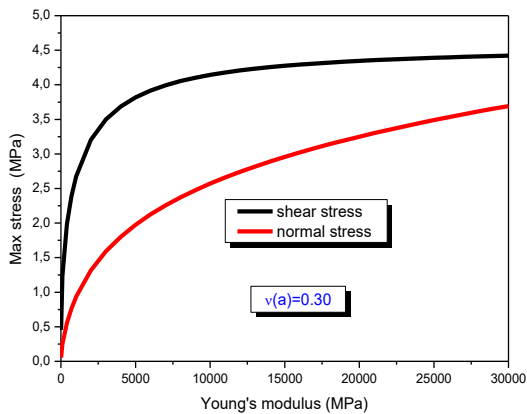


Fig. 5 Interfacial maximum stress versus Young's modulus of adhesive for Poisson's ratio  $\nu_a=0.30$

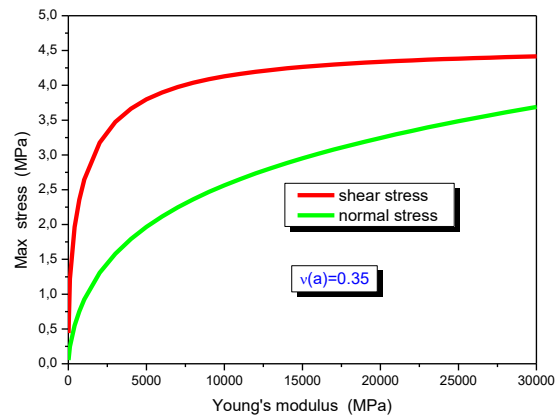


Fig. 6 Interfacial maximum stress versus Young's modulus of adhesive for Poisson's ratio  $\nu_a=0.35$

the present solution gives results which generally agree better with those from Smith's and Teng 2001, Yang's and Wu 2007, Tounsi's 2006, Hassaine Daouadji's 2013 solutions. The latter two again give similar results. In short, it may be concluded that all solutions are satisfactory for RC beams bonded with a thin plate as the rigidity of the soffit plate is small in comparison with the that of the RC beam. Those solutions which consider the additional bending and shear deformations in the soffit plate due to the interfacial shear stresses give more accurate results. The present solution is the only solution which covers the uniformly distributed loads and considers this effect and the effects of other parameters.

#### 4.3 Parametric studies

For each of the five Poisson's ratios of the adhesives, results for edge stresses, corresponding to various Young's modulus of adhesive  $E_a$ , ranging between 0.001 and 30 GPa are presented in graphical forms.

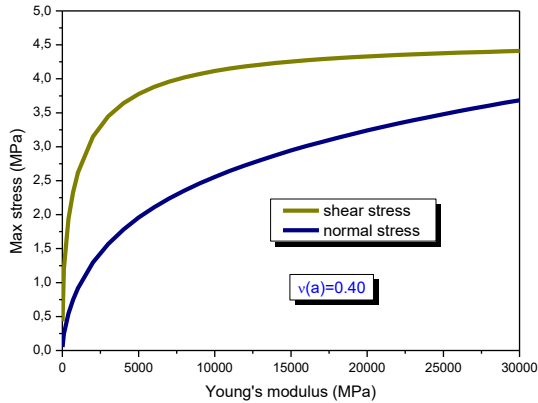


Fig. 7 Interfacial maximum stress versus Young's modulus of adhesive for Poisson's ratio  $v_a=0.40$

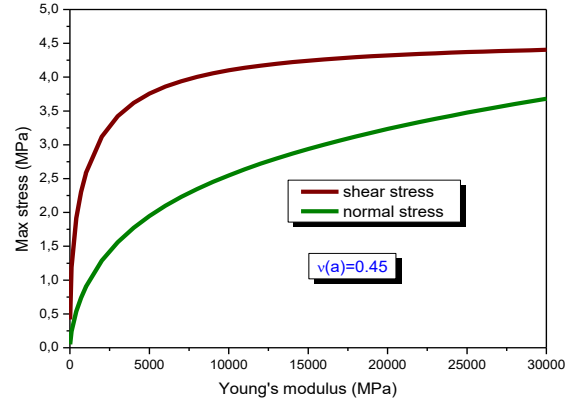


Fig. 8 Interfacial maximum stress versus Young's modulus of adhesive for Poisson's ratio  $v_a=0.45$

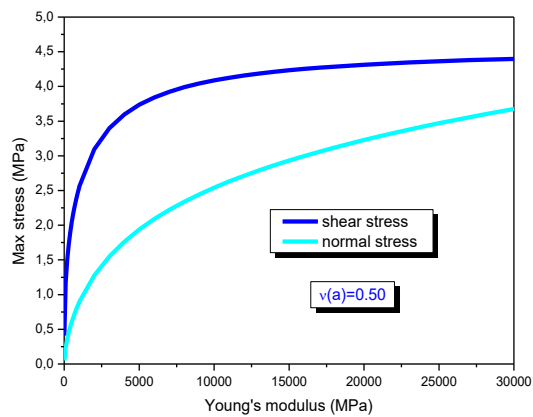


Fig. 9 Interfacial maximum stress versus Young's modulus of adhesive for Poisson's ratio  $v_a=0.50$

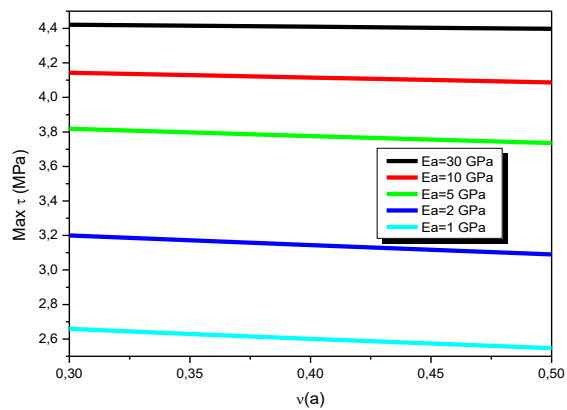


Fig. 10 Interfacial maximum shear stress versus Poisson's ratio of adhesive

#### 4.3.1 Effect of Young's modulus

The two edge stresses (shear and normal stress) corresponding to Poisson's ratio  $v_a=0.3$  are shown in Fig. 5. From Fig. 5, it is seen that both shear and normal interfacial stress increase gradually as the Young's modulus of adhesive increase from 0.001 to 30 GPa. Figs. 6 to 9 show that when Poisson's ratio  $v_a=0.35, 0.4, 0.45$  and  $0.5$ , similar variations of the maximum interfacial stress with Young's modulus as in the case of  $v_a=0.3$  (Fig. 5) are obtained. The interfacial stresses shown in Fig. 5 for Poisson's ratio  $v_a=0.3$  and Young's modulus,  $E_a$ , greater than 5 GPa are representative of those that will be obtained when very hard adhesives such as ceramic glue are used. Similarly, the interfacial stresses shown in Figs. 6 and 7 for Poisson's ratios  $v_a=0.35$  and  $0.4$  and for Young's modulus,  $E_a$ , within the range 0.05-5 GPa apply to adhesives comprising of multiple part epoxies. On the other hand, the interfacial stresses shown in Figs. 8 and 9 for Poisson's ratios  $v_a=0.45$  and  $0.5$  and for Young's modulus,  $E_a$ , less than 0.05 GPa are representative of those manifested by rubber-like or elastomeric adhesives.

#### 4.3.2 Effect of Poisson's ratio

The two maximum adhesive stresses (shear and normal stress) versus Poisson's ratio of adhesive for different value of Young's modulus of adhesive ( $E_a=1, 2, 5, 10$  and  $30$  GPa) are shown in Fig. 10. It can be seen from the presented results that the Poisson's ratio of adhesive has almost no effect on the variation of the maximum adhesive stresses. However, these stresses increase gradually with the Young's modulus of adhesive. We note that the adhesives with Young's modulus smaller than  $1$  GPa are not commonly used in practice. In addition, the adhesives with Young's modulus  $E_a=30$  GPa is used only for theoretical comparison.

## 5. Conclusions

A systematic rigorous general approach for the analysis of interfacial stresses in steel beams strengthened with externally bonded hygrothermal aged FRP plate has been presented. This approach is based on elastic foundation model in which the adherend shear deformations have been included by assuming a linear shear stress through the depth of the steel beam. By comparing with experimental results, the present closed-solution provides satisfactory predictions to the interfacial shear stress in the plated beams. The influence of adhesive properties on the adhesive stresses in beams strengthened with FRP plates has been investigated using an improved analytical model. The adherend shear deformations are taken into account by assuming a parabolic shear stress through the thickness of both the steel beam and bonded plate. By comparing with experimental results, the present closed-solution provides satisfactory predictions to the interfacial shear stress in the plated beams. The maximum interfacial stresses have been analysed using adhesives of various Young's modulus and Poisson's ratio properties. In general, the maximum interfacial stress increase with an increase in the Young's modulus of adhesive, but does not appear to change significantly with an increase in the Poisson's ratio.

In conclusion, we can say that in addition to matrix composite fiber materials, another alternative may be proposed for strengthening structures, this will involve the use of functionally graded materials FGM (Abdelhak *et al.* 2015, Tounsi *et al.* 2013, Benferhat *et al.* 2015, Bourada *et al.* 2015, Belabed *et al.* 2014, Hassaine Daouadji 2013, Hebali *et al.* 2014, Ait yahia *et al.* 2015, Ait amar *et al.* 2014, Bennoun *et al.* 2016, Zidi *et al.* 2014, Bouderra *et al.* 2013, Tounsi *et al.* 2013, Bousahla *et al.* 2014) in order to ensure continuity properties lift through the thickness of the reinforcement plate.

## Acknowledgments

The author thanks the referees for their helpful comments.

## References

- Ait Amar Meziane, M., Tounsi, A. and Abdelaziz, H. (2014), "An efficient and simple refined theory for buckling and free vibration of exponentially graded sandwich plates under various boundary conditions", *J. Sandw. Struct. Mater.*, **16**(3), 293-318.
- Ait Yahia, S., Ait Atmane, H., Houari, M.S.A. and Tounsi, A. (2015), "Wave propagation in functionally

- graded plates with porosities using various higher-order shear deformation plate theories”, *Struct. Eng. Mech.*, **53**(6), 1143-1165.
- Belabed, Z., Houari, M.S.A., Tounsi, A., Mahmoud, S.R. and Anwar Bég, O. (2014), “An efficient and simple higher order shear and normal deformation theory for functionally graded material (FGM) plates”, *Compos. Part B*, **60**, 274-283.
- Bennoun, M., Houari, M.S.A. and Tounsi, A. (2016), “A novel five variable refined plate theory for vibration analysis of functionally graded sandwich plates”, *Mech. Adv. Mater. Struct.*, **23**(4), 423-431.
- Benyoucef S., A.Tounsi, R.Yeghnem, B. Bouiadjra, and E.A.Adda Bedia (2014), “An analysis of interfacial stresses in steel beams bonded with a thin composite plate under thermomechanical loading”, *Mech. Compos. Mater.*, **49**, 959-972.
- Bouakaz K., Hassaine Daouadji, T., Meftah, S.A., Ameer, M., Tounsi, A. and Adda Bedia, E.A. (2014), “A Numerical analysis of steel beams strengthened with composite materials”, *Mech. Compos. Mater.*, **50**(4), 685-696.
- Bouderba, B., Houari, M.S.A. and Tounsi, A. (2013), “Thermomechanical bending response of FGM thick plates resting on Winkler-Pasternak elastic foundations”, *Steel Compos. Struct.*, **14**(1), 85-104.
- Bourada, M., Kaci, A., Houari, M.S.A. and Tounsi, A. (2015), “A new simple shear and normal deformations theory for functionally graded beams”, *Steel Compos. Struct.*, **18**(2), 409-423.
- Bousahla, A.A., Houari, M.S.A., Tounsi, A. and Adda Bedia, E.A., (2014), “A novel higher order shear and normal deformation theory based on neutral surface position for bending analysis of advanced composite plates”, *Int. J. Comput. Meth.*, **11**(6), 1350082.
- El Mahi, Benrahou, K.H., Belakhdar, Kh., Tounsi, A. and Adda Bedia, El A. (2014), “Effect of the tapered of the end of a FRP plate on the interfacial stresses in a strengthened beam used in civil engineering applications”, *Mech. Compos. Mater.*, **50**(4), 465-474.
- Guenaneche, B., Tounsi, A. and Adda Bedia, E.A. (2014), “Effect of shear deformation on interfacial stress analysis in plated beams under arbitrary loading”, *Adhes. Adhes.*, **48**, 1-13.
- Hassaine Daouadji, T. (2013), “Analytical analysis of the interfacial stress in damaged reinforced concrete beams strengthened by bonded composite plates”, *Streng. Mater.*, **45**(5), 587-597.
- Hebali, H., Tounsi, A., Houari, M.S.A., Bessaim, A. and Adda Bedia, E.A. (2014), “A new quasi-3D hyperbolic shear deformation theory for the static and free vibration analysis of functionally graded plates”, *J. Eng. Mech.*, ASCE, **140**, 374-383.
- Herakovich, C.T. (1998), *Mechanics of fibrous composites*, John Wiley & Sonc, Inc., USA.
- Jones, R., Swamy, R.N. and Charif, A. (1988), “Plate separation and anchorage of reinforced concrete beams strengthened by epoxy-bonded steel plates”, *Struct. Eng.*, **66**(5), 85-94.
- Krou, B., Bernard, F. and Tounsi, A. (2013), “Fibers orientation optimization for concrete beam strengthened with a CFRP bonded plate: A coupled analytical-numerical investigation”, *Eng. Struct.*, **9**, 218-227.
- Oller, E., Marí, A., Bairán, J. and Cladera, A. (2015), “Shear design of reinforced concrete beams with FRP longitudinal and transverse reinforcement”, *Compos. Part B: Eng.*, **74**, 104-122.
- Smith, S.T. and Teng, J.G. (2001), “Interfacial stresses in plated beams”, *Eng. Struct.*, **23**(7), 857-71.
- Touati, M., Tounsi, A. and Benguediab, M. (2015), “Effect of shear deformation on adhesive stresses in plated concrete beams: Analytical solutions”, *Comput. Concrete*, **15**(3), 141-166
- Tounsi, A. (2006), “Improved theoretical solution for interfacial stresses in concrete beams strengthened with FRP plate”, *Int. J. Solid. Struct.*, **43**(14-15), 54-74.
- Tounsi, A., Benyoucef, S. and Adda Bedia, E.A. (2009), “Interfacial stresses in FRP-plated RC beams: Effect of adherend shear deformations”, *Int. J. Adhes. Adhes.*, **29**, 343-351
- Tounsi, A., Houari, M.S.A., Benyoucef, S. and Adda Bedia, E.A. (2013), “A refined trigonometric shear deformation theory for thermoelastic bending of functionally graded sandwich plates”, *Aerosp. Sci. Tech.*, **24**, 209-220.
- Tsai, M.Y., Oplinger, D.W. and Morton, J. (1998), “Improved theoretical solutions for adhesive lap joints”, *Int. J. Solid. Struct.*, **35**(12), 1163-85.
- Yang, J. and Wu, Y.F. (2007), “Interfacial stresses of FRP strengthened concrete beams: effect of shear

- deformation”, *Compos. Struct.*, **80**, 343-351.
- Zidani, M.B., Belakhdar, K., Tounsi, A. and Adda Bedia, E.A. (2015), “Finite element analysis of initially damaged beams repaired with FRP plates”, *Compos. Struct.*, **134**, 429-439.
- Zidi, M., Tounsi, A., Houari, M.S.A., Adda Bedia, E.A. and Anwar Bég, O. (2014), “Bending analysis of FGM plates under hygro-thermo-mechanical loading using a four variable refined plate theory”, *Aerosp. Sci. Tech.*, **34**, 24-34.

CC